

INTERCONNECTION TECHNOLOGY IN ELECTRONIC PACKAGING AND ASSEMBLY

by Chunqing Wang, Mingyu Li and Yanhong.Tian

National Key Laboratory of Advanced Welding Production Technology,
P.O. Box 436, Harbin Institute of Technology, Harbin 150001, China, wangcq@hope.hit.edu.cn

ABSTRACT

This paper reviews our recent research works on the interconnection technologies in electronic packaging and assembly. At the aspect of advanced joining methods, laser-ultrasonic fluxless soldering technology was proposed. The characteristic of this technology is that the oxide film was removed through the vibration excited by high frequency laser change in the molten solder droplet. Application researches of laser soldering technology on solder bumping of BGA packages were carried out. Furthermore, interfacial reaction between SnPb eutectic solder and Au/Ni/Cu pad during laser reflow was analyzed. At the aspect of soldered joints' reliability, the system for predicting and analyzing SMT solder joint shape and reliability(PSAR) has been designed. Optimization design method of soldered joints' structure was brought forward after the investigation of fatigue failure of RC chip devices and BGA packages under temperature cyclic conditions with FEM analysis and experimental study. At the aspect of solder alloy design, alloy design method based on quantum was proposed. The macroproperties such as melting point, wettability and strength were described by the electron parameters. In this way, a great deal of the experimental investigations was replaced, so as to realize the design and research of any kinds of solder alloys with low cost and high efficiency.

KEYWORDS

laser-ultrasonic fluxless soldering, BGA laser reflow; solder joint shape and reliability, solder alloy design

1.Introduction

The interconnection technology is the key to the electronics packaging and assembly. It has been regarded that joining methods and reliability of solder joint as well as materials are the soul and the heart of the microelectronics industry. In recent years, much attention has been paid to the pollution-free technology in the production and the high reliability of solder joint. In the prevalent solder interconnection technology, the erosion caused by the residual flux near the joints and the electric iron dissociated from the moist air have bad influence on the reliability of the fine-pitch solder joints and the insurability of electronic circuits. To solve this question freon abluent is used to clean the solder joints. But the freon abluent will spoil the ozonosphere and pollute the earth environment. So the fluxless soldering technology free from cleaning and erosion in the joints attracted much concern. In addition, laser reflow is becoming a potential technique for solder bumping in the area of electronics manufacturing due to its excellent characteristics such as high energy input and local heating capability, which makes it a good candidate for solder bumping in plastic ball grid array(PBGA) packages.

The reliability of solder interconnection joint is also one focal subject in the development of microelectronics packaging and assembly technology. Solder joint shape is one of critical factor to influence the reliability. To integrate the predication of solder joint shape and the analysis of the reliability have a greater significant in theory and also in practice. We have carried out some work, it is to perfect the research on solder joint shape predication ,mechanical performance analysis and thermal fatigue life prediction.

Sn-based solders have been the most important material for the mounting and packaging of electronic

components. Traditional experiments are still the normal rule in developing Sn-based solders. However, it is both time consuming and expensive to carry out an uncertain experiment. The computational method should be an important direction in material designing in view of inexpensive cost, high efficiency and prediction. The developments in quantum theory, solid physics and computational methods make it feasible for us to carry out research on Sn-based solder alloys by means of calculation.

2. Laser Reflow Soldering

2.1 Fluxless Laser Soldering

Mingyu Li et al performed fluxless laser soldering in the low vacuum environment (the vacuum degree is 8Pa) with Nd:YAG laser[1,2]. Eutectic 63Sn/37Pb solder balls with 1mm diameter were used and the square Cu-pads on a resin substrate were 0.03mm thick. The laser generator improved by the authors can provide continuous laser and modulated laser with beam diameter of 0.7mm.

The experiment utilized two kind of laser heating source (continuous laser and modulated laser) to heat the solder on the pad in order to observe, compare and analyze the wetting effect of the solder drop. The results indicate the the Cu-pad can not be wetted by the solder whatever adjustment of the laser input energy when heated by the continuous laser under the condition of vacuum level less than 8Pa. In this case, it is difficult to perform the fluxless soldering. However, the surface of the Cu-pad can be wetted by the solder being heated by the ultrasonic (20kHz) modulated laser in the wider range of the laser input energy. Fig.1 shows the wetting effect of solder drop being heated by the continuous laser and modulated laser. It can be seen that the wetting angle is as high as 145° with continuous laser, and the wetting angle is about 25° with modulated laser .

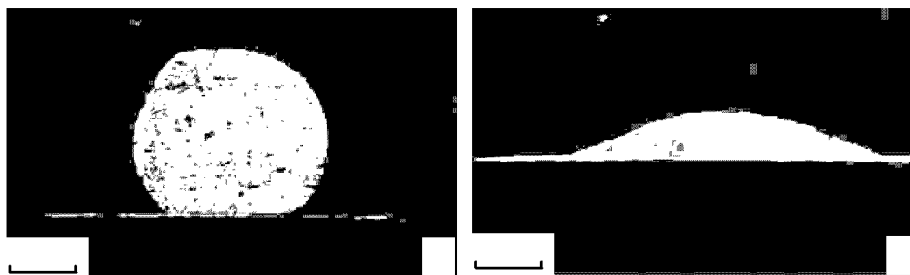


Fig.1 Wetting effect of solder drop being heated by (a) continuous laser and (b) modulated laser.

In the experiment the laser applied is gained by modulating the continuous laser forcefully. Because the laser heats the solder in the impulse pattern, the output energy is bigger and the heating time is longer. The experimental result shows that there is a sharp contrast between the solder wetting effect in the heat of the ultrasonic modulated laser and that of the continuous laser. The ultrasonic modulated laser plays a positive role in accelerating the solder wetting on the pad, and fluxless solder can be achieved with ultrasonic modulated laser. This method is defined as fluxless soldering under the heat of ultrasonic modulated laser.

Numerical simulation on temperature distribution of the solder drop was carried out to investigate the mechanism of solder wetting forced by the ultrasonic modulated laser[xxx]. Figure2 was the modeling results of temperature change of the solder drop (the laser power is 14W, the duty ratio of impulse is 1:1, the frequency is 20kHz).

The curve a、 b、 c、 d shown in Fig.2 represent the temperature change at the point a、 b、 c、 d of the solder drop. The calculating results suggest that the surface of solder drop in heat of ultrasonic modulated laser generated synchronous temperature field, the range of which is about 3°C . The oscillating temperature field distributes on the heating surface of the solder rather than inside of the solder. According to the heat-transfer theory, this method is caused by the thermal inertia of the heating source in the process of heat transfer. The author defined this phenomenon as the oscillation effect of the surface temperature in heat of high-frequency

laser. According to the principle of thermodynamics, the ultrasonic oscillation can be generated at the solder drop surface in the function of the ultrasonic-oscillating temperature field. In order to prove the conclusion, on the basis of the temperature field analyzing, the laser interferometer (Polytec OFV502) was applied to observe the oscillating phenomenon of the solder drop surface heated by ultrasonic modulated laser. Fig.3 is the testing result of the oscillation at the solder drop surface. The mechanical oscillation was found at the solder drop surface heated by laser, and the range of oscillation is $0.3\mu\text{m}$. The mechanical oscillation frequency at the solder drop surface is 20kHz, which coincides with the modulated frequency of laser and the frequency of the temperature field oscillation at the solder drop surface generated by the laser. Thus, it can be considered that the temperature oscillation at the solder drop surface is generated when heated by the ultrasonic modulated laser, and the ultrasonic mechanical oscillation at the solder drop surface is generated due to the thermodynamic effect of the object.

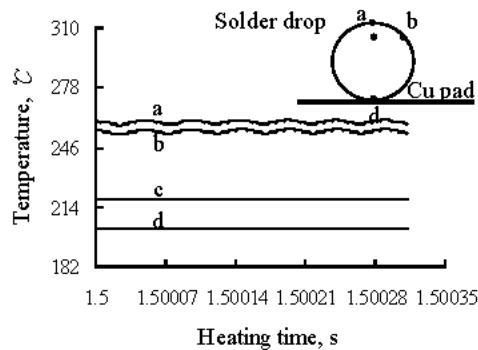


Fig.2 Temperature change of solder drop in the heat of modulated laser ($P=14\text{W}$, Duty ratio=1:1, $f=20\text{kHz}$)

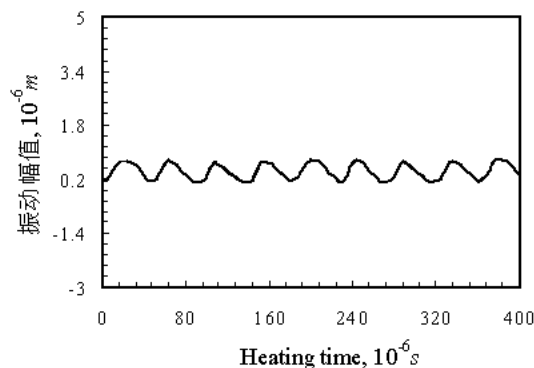


Fig.3 Testing result of solder drop surface oscillation ($P=14\text{W}$, Duty ratio=1:1, $f=20\text{kHz}$)

The sound wave pressure at the interface of the solder and the pad was also numerically calculated according to the wave-transfer theory to investigate the wetting effect. Fig.4 was the calculating result of the transmission of the sound wave pressure at the interface of the Sn/Pb solder and the Cu-pad when heated by the modulated laser (the laser power is 14w, the duty ratio of impulse is 1:1, the frequency is 20kHz). It can be seen that the pressure variation is generated at the interface of the solder and the pad. Negative pressure appears in particular condition. According to ultrasonic cavitation theory, tearing force and the vacuolar can be generated in the negative pressure region. Then the vacuolar will break in the compressing force to generate strong shock wave.

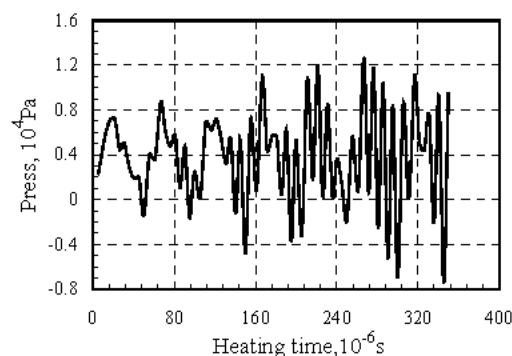


Fig.4 Pressure change of the solder wetting interface being heated by the ultrasonic modulated laser

The proceeding theoretical analysis and the experimental results indicate that the reason of the Sn/Pb solder wetting on the Cu-pad forced by the ultrasonic modulated laser (et. Ultrasonic oscillation is generated at the

solder drop surface when heated by the ultrasonic modulated laser. As the ultrasonic oscillation at the solder drop surface transmits to the interface of the solder and Cu-pad, strong shock wave is generated. The shock wave can break the oxide in the interface for the solder to wet effectively). Compared with other fluxless soldering methods, the traits of fluxless soldering under the heat of ultrasonic modulated laser are as follows: utilizing the property of laser, local heat of the joint can be achieved; particular reducing technology is not needed, the self-excited ultrasonic cavitation can break the oxide; ultrasonic machine is not in use. The ultrasonic cavitation is generated by the none-contact photo-thermal effect of laser; noble metal for protection is not in use.

2.2 PBGA Laser Reflow

Laser reflow is a potential technique in solder bumping of PBGA packages. Our previous studies performed the laser reflow bumping of 63Sn37Pb eutectic solder balls (dia. of 0.76 mm) on the Au/Ni plated BT substrates [3,4]. The thin top Au layer is about 2 μm thick. Interfacial reaction between eutectic solder and Au/Ni/Cu metallization was also analyzed. The laser device was a continuous wave type Nd: YAG laser with a beam diameter 0.6mm. Fig.5 shows surface morphology and cross section of solder bump reflowed by laser. It can be seen that solder bump with smooth surface can be formed with appropriate laser power within short laser heating time. No soldering defect was found at the solder/pad interface, seen from Fig.5b. Also, the microstructure inside the solder bump was fine and uniform. The results of ball shear test showed that the shear strength of solder bump reflowed by laser is higher than the bump reflowed by hot air.

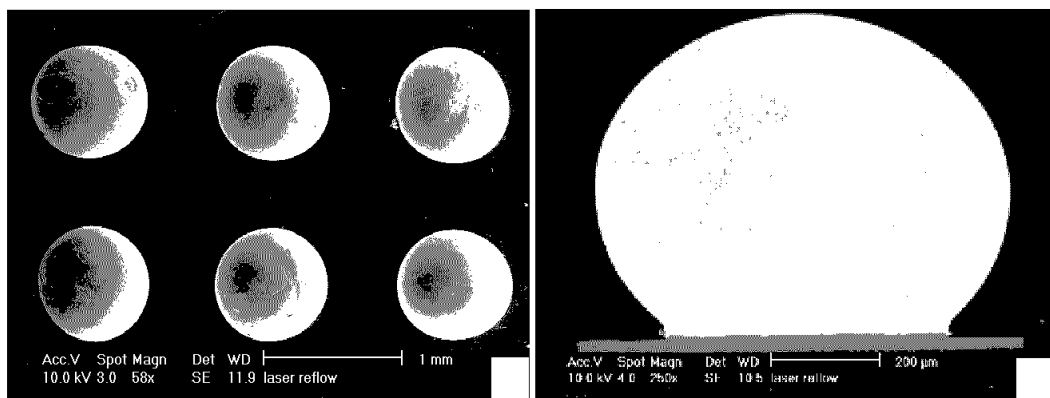


Fig.5 Solder bump reflowed by laser for 0.05s under 25W

(a) Surface morphology of solder bumps; (b) Cross section of solder bump;

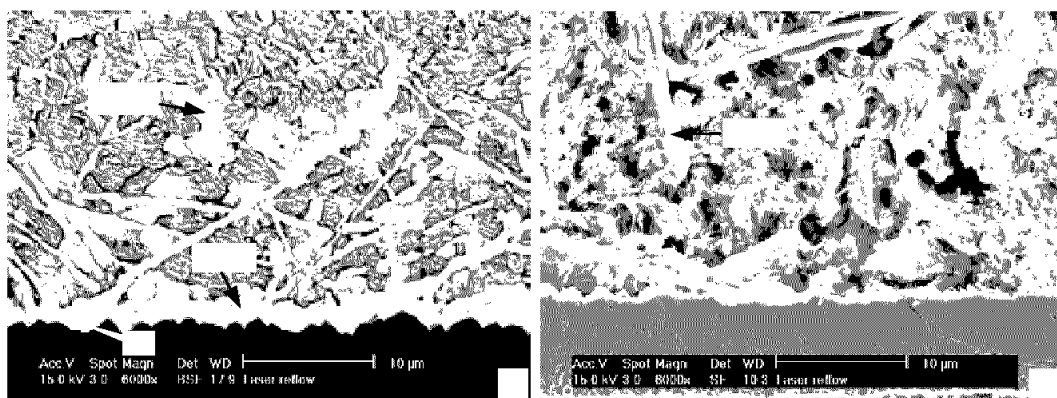


Fig.6 SEM images of the solder bump interface (a) 0.2s, 15W, (b) 0.5s, 15W

Fig.6 showed the SEM images of the solder bump interface reflowed by different laser input energy. When

using a 15 W laser power heating for 0.2s, a continuous intermetallic compound layer (a few μm thick) and needle-like intermetallics formed at the solder joint. A layer of Au layer remained at the solder/pad interface (Fig. 6a) . The needle-like phases grew sidewise from the continuous intermetallic layer at the solder/pad interface into the solder, and then spread out to the entire interface region. EDX analysis on the continuous intermetallic layer and needle-shape intermetallics indicate that the intermetallics were AuSn_4 . When the eutectic solder ball was melted by the laser and contacted with the Au/Ni/Cu pad, the Sn in the molten solder reacted with Au to form a continuous AuSn_4 layer at the interface and then the needle-like AuSn_4 formed above the layer. The formation of this needle-like compound was due to rapid cooling rate by the laser heating nature, and its preferred growth direction of AuSn_4 was greatly controlled by the fast cooling direction. The remaining Au at the Ni/intermetallic interface indicates that the Au layer in the pad did not react completely because of the short laser heating time. In Fig.6a, it could also be found that at least a 2 μm thick layer of AuSn_4 was formed within 0.2s laser heating time. Under a 15 W laser power and heating for 0.5s, both the continuous AuSn_4 layer and needle-like AuSn_4 disappeared at all at the interface. Instead, rod-shaped AuSn_4 was found in the solder matrix, as shown in Fig.6b.

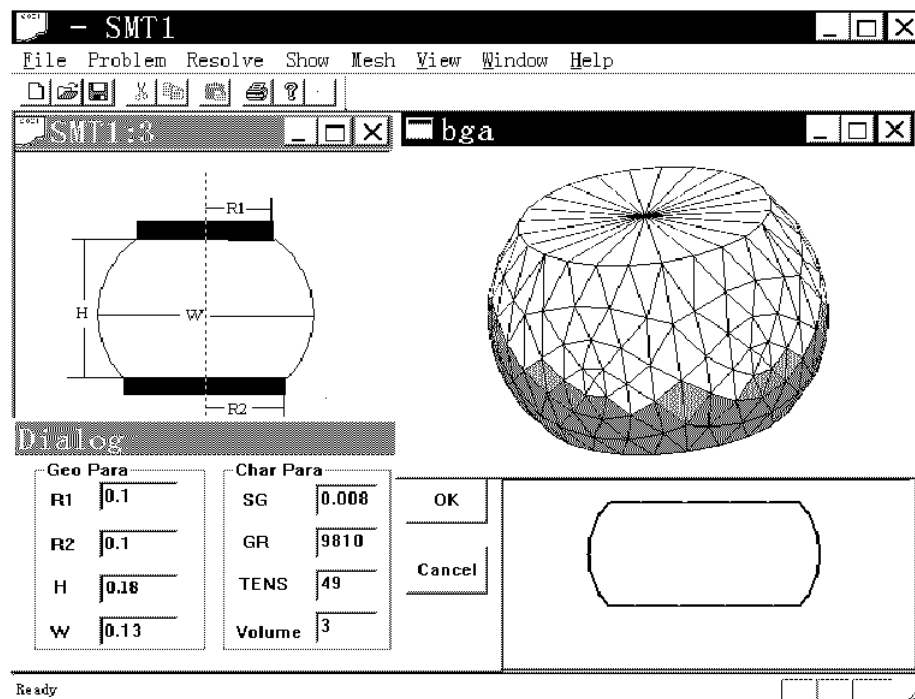
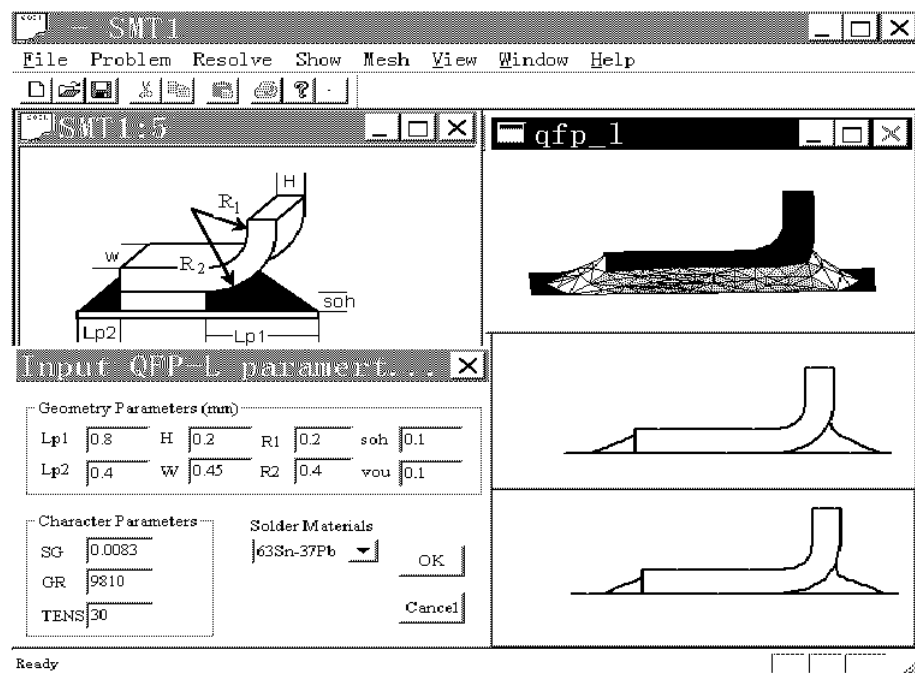
Based on the above observations, a series of interfacial reactions might occur within a short laser heating time. Firstly, Sn in the molten solder could react with Au to form a continuous AuSn_4 layer, and needle-like AuSn_4 would initiate and grow on the continuous intermetallic layer due to high temperature gradient. Secondly, needle-like AuSn_4 intermetallics might break off from the interface during the solidification of the molten solder. With an increase of the laser input energy, the needle-like AuSn_4 phase could break off into the solder bulk, forming random distribution of AuSn_4 rods within the whole solder bump. Finally, AuSn_4 rods would dissolve into the solder matrix.

3.Reliability of Solder Joints

3.1 The predication of solder joint shape

Our previous studies developed an integrated system for predicting and analyzing SMT solder joint shape and reliability(PSAR).[5,6] The system is based on Windows/NT system using object-oriented approach. A three-dimensional finite element program Surface Evolver is incorporated to calculate the shape of solder joints based on minimum potential energy theorem. A preprocessor is developed in which the potential energy, geometry of the conjunction and boundary conditions of the initial joint can be specified using a visual method and transferred into Evolver syntax automatically. A post processor is built to treat the result from Evolver and generate automatically a program which can serve as a preprocessor for finite element joint analysis program ANSYS. In addition, a comprehensive material database and a standard component database are developed and implemented. The formation of solder joint generally involves a reflow process to heat a solder paste placed at the junction of the component and board until the solder in the paste liquefies. The liquid solder wets and spreads along the solid surface and then cools to form the characteristic solid joint between the component and the board, the component is thus joined with the pad. Ignoring the contraction of solder volume in the process of solidification, the final shape of solder joint is considered to be the static equilibrium shape of the molten solder formed at the conjunction, when the total potential energy consisted in the component- pad - molten solder-gas system of a solder joint is minimized.

Fig.7 and Fig.8 are displays of predicting the shape of QFP_L and BGA joints in multiple windows. The left upper window is the compilation window and the left bottom window is the dialog window, which show the initial joint graph and process parameters of the joint respectively. The right upper window shows the global joint shape of the joint, and the right bottom window shows the sectional shape.



3.2 Mechanical Analysis of Solder Joints in Thermal Cycle

A solid model is needed to analyze the mechanical behavior of the solder joint using ANSYS/Multiphysics program. The datum about the nodes and elements in the surface of the solder joint output from Evolver are obtained, and combined with the datum about the geometrical profile of the component and pad into the special datum that ANSYS needs to build the solid model. The teeny elements are dispelled and the discrete elements are revised. Thus, the whole mechanical analysis model of solder joints is generated.

An elasto-plasto-creep material model is established and its mechanical constitutive equation is given as following:

$$\dot{\varepsilon}_{ij} = \frac{1+\nu}{E} \dot{\sigma}_{ij} - \frac{\nu}{E} \dot{\sigma}_{kk} \delta_{ij} + 3\alpha\varepsilon_0 \frac{\dot{\sigma}_i}{\sigma_0^2} S_{ij} + \frac{3}{2} D \sigma_i^{n-1} e^{\left(\frac{-Q_0}{RT}\right)} S_{ij} \quad (1)$$

where E , α , ε_0 , σ_0 —Temperature dependent material properties parameters

Material properties 63Sn37Pb with the variation of temperature, are defined in the material database, according to experiments or relevant references. The applied loading on the solder joint in the mechanical analysis consists of 36°C temperature ramps in one minute with 10 minutes at the extreme temperatures, the whole temperature range of -55°C~+125°C and two cycles in one hour. It can be seen in the Fig.9 shows the distribution of internal stress and strain in the RC solder joint at the start and end point of the extreme low and high temperature range.

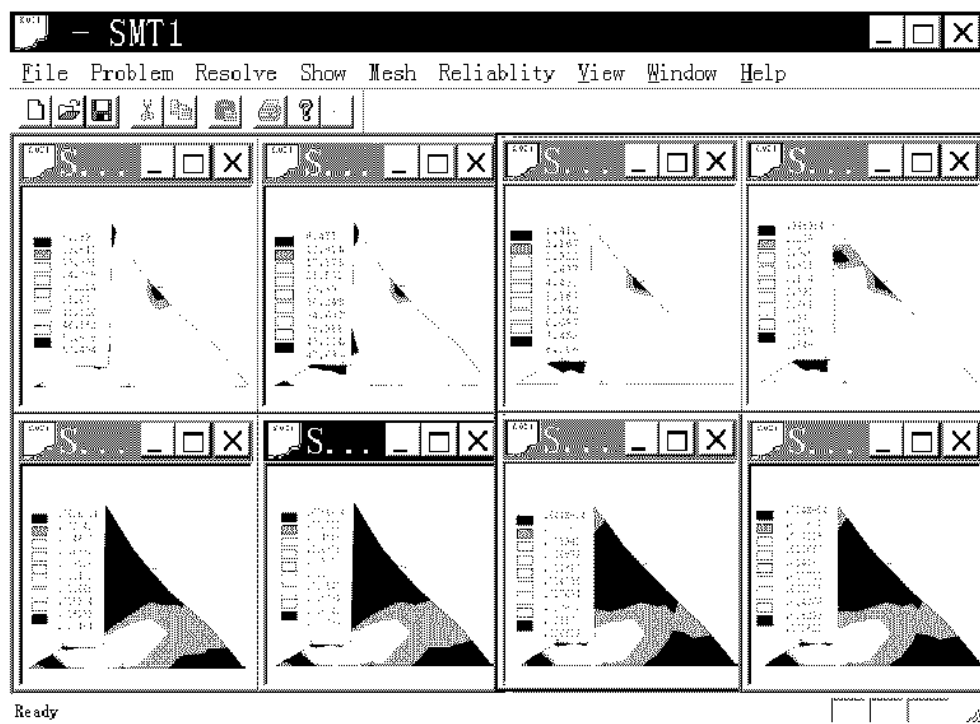


Fig.9 The distribution of the internal stress and strain in solder joint

3.3 The predication of fatigue life

In the PSAR system, a Manson-Coffin equation revised by Engelmaier is used to predict the fatigue life of the RC chip solder joint. For SnPb solder, the relation between the fatigue life and the equivalent total strain difference is given:

$$N_f = \frac{1}{2} \left(\frac{\Delta\gamma}{2\varepsilon'_f} \right)^{1/c} \quad (2)$$

where N_f —the mean number of cycles to failure; $\Delta\gamma$ —cyclic shear strain difference; ε'_f —the fatigue ductility coefficient; $c=0.325$.

The hysteresis loops of stress-strain in the solder joint predicted by ANSYS is shown in Fig.10. Because the loops tend to be invariable after first several cycles, the total shear strain difference in first four cycles is used to

predict the fatigue life of the solder joint.

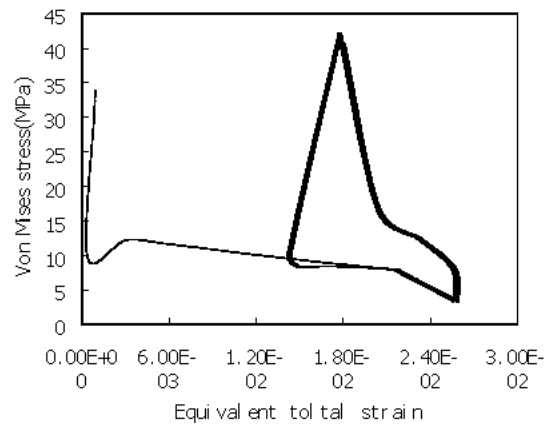


Fig.10 Hysteresis loops of stress-strain in the solder joint

Table.1 Predicted solder joint shape and reliability with various structural parameters

number	Lp(mm)	Soh(mm)	V(mm ³)	shape	($\Delta\gamma \times 10^{-3}$)	Nf
v1	0.7	0.1	0.25	concave	1.84	4125
v2	0.7	0.1	0.35	flat	1.13	14122
v3	0.7	0.1	0.5	slightly convex	1.26	10920
s1	0.7	0.0	0.35	convex	2.33	2284
s2	0.7	0.05	0.35	convex	1.76	4646
s3	0.7	0.2	0.35	concave	1.08	15996
l1	0.4	0.1	0.35	convex	1.11	14924
l2	0.6	0.1	0.35	flat	1.21	11996
l3	0.8	0.1	0.35	concave	1.18	12783

Table.1 is the result of predicting the shape and fatigue life of the solder joint using PSAR system. It can be seen that when the pad extension(Lp) and stand-off height(soh) are constant, with the increment of solder volume(V), the solder joint changes from concave to slightly convex type, and the fatigue life of the solder joint increases. But with solder volume goes on increasing, the solder joint shape changes to heavily convex and the fatigue life of the solder joint decrease. When the pad extension and solder volume are constant, with the increment of stand-off height, the fatigue life of the solder joint increases. But with stand-off height goes on increasing, the solder joint shape changes from convex to concave and the fatigue life increases little. So, increasing soh in a certain range can improve the solder joint reliability while higher soh does little contribution to the reliability. It is enough with the soh slightly higher than 0.1mm for RC1206. When solder volume and stand-off height are constant, with the increment of pad extension, the fatigue life of the solder joint increases, but changes little. So, it is enough to keep pad extension slightly higher than the height of the solder joint. From the above predicted results, it can be concluded that the solder joint with approximately flat shape has high reliability.

4 Design of Solder Alloys

4.1 Electron Structure of Sn-based Solder Alloys

In view of microscopic interaction, alloying effects and properties of Sn-based solder alloys should depend on the interaction of all the atoms contained in the solder. In other words, the states of electronic structure formed through

the interaction of atoms will essentially determine the properties of Sn-based solder alloys. Consequently, it is a fundamental issue to understand the properties of solder alloys at the atom or electron level by calculating the corresponding electronic states and finding the intrinsic relationships between electronic parameters and properties of solder alloys.

Feng WF et al. designed an Sn_{28}M ($\text{M} = \text{Cu}, \text{Zn}, \text{Ga}, \text{Ge}, \text{As}, \text{Ag}, \text{Cd}, \text{In}, \text{Sn}, \text{Sb}, \text{Au}, \text{Hg}, \text{Tl}, \text{Pb}$ and Bi) cluster model[7,8]. It was based on the crystal structure of β -Sn, as shown in Fig.11. It was made up of an alloying atom M ($\text{M} = \text{Zn}, \text{Ag}, \text{Cd}, \text{In}, \text{Sn}, \text{Sb}, \text{Pb}$ and Bi etc.) at center and 28 surrounding Sn atoms. The lattice parameters used in the present calculation were $a = 0.58197$ nm and $c = 0.31750$ nm. There are four first-nearest-neighbor atoms and two second-nearest-neighbor atoms around M atom. Moreover, four first-nearest-neighbor atoms surrounded each first-nearest-neighbor atom. The distance between an atom and its first-nearest-neighbor atom is 0.302nm. The distance between an atom and its second-nearest-neighbor atom is 0.318nm. Then, some electronic parameters such as ionicity, Mk (s orbital energy level beyond Fermi energy) and Bo (the orbital interaction) were obtained through the relativistic DV- $X\alpha$ calculation.

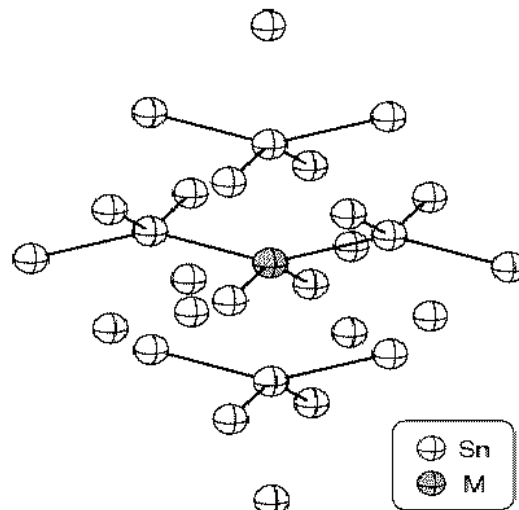


Fig.11 Cluster Model Sn_{28}M for Calculating alloying effects

4.2 Prediction of Wettability of Solder Alloys

Five octahedron clusters were set up to understand wettability of Sn-based solder alloys, which were applied in modern electronic mounting and packaging[xxxx]. Because heavy atoms such as Pb, Bi, Sn and Sb were included in our clusters, relativistic effects were taken into account in the calculation in order to obtain exact results. The existence of alloying atom M would result in the change of orbital interaction between atoms, which would result in the improvement or decline of wettability. Fig.12 shows octahedron clusters for wettabilities of Sn-based solders

To a great extent, the wettability of Sn-based solder on Cu substrate depends on the interaction between Sn atom and Cu atom. Observing the effects of alloying elements on the wettability of Sn-based solders, we found alloying element M that had strong orbital interaction with Sn and had weak even little orbital interaction with Cu, such as Pb, Bi and Ag, could enforce the wettability because M increased the orbital interaction between Sn atom Cu atom. On the contrary, Alloying element M that had strong orbital interaction with both Sn and Cu or had relative weak orbital interaction with Sn, such as Sb, Cd and Zn, could decline the wettability because M decreased the orbital interaction between Sn atom Cu atom. Specially, although element In had both relative strong orbital interaction with Sn and Cu atom, Sn/In solders could spread well on Cu substrate because In

increased the orbital interaction between Sn and Cu. It is believed that the wettability of Sn-based solder on Cu would be improved only if orbital interactions between Sn atoms and Cu atoms are enforced because of the existence of M element.

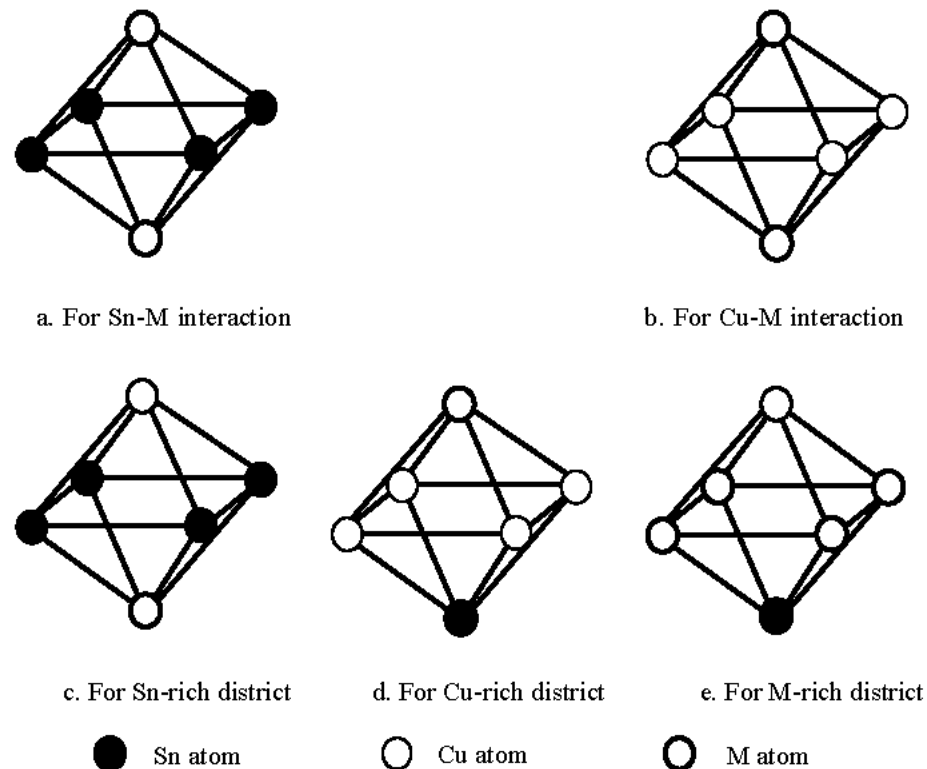


Fig.12 Octahedron clusters for wettabilities of Sn-based solders

Parameter B_0 was obtained through relativistic DV-X α calculation and Mulliken analysis. Then electronic structure mechanism for the wettability of Sn-based solder alloys on Cu substrate was put forward based on the analysis of orbital interactions between atoms. It is believed that the wettability of Sn $_x$ M $_y$ alloy would be improved only if orbital interactions between Sn atoms and Cu atoms are enforced because of the existence of M element. Predictions from analysis on calculation results were proved by both spreading and wetting behavior experiments and EDX analysis. The wettability mechanism was put forward for the first time at the electronic level.

5. Conclusions

1. Laser-ultrasonic fluxless soldering technology was realized by modulating the laser to a high frequency to remove the oxide film through the vibration.
2. Laser reflow was successfully applied on the solder bumping of PBGA solder ball with high quality solder bump.
3. The system for predicting and analyzing SMT solder joint shape and reliability(PSAR) was designed.
4. A new method for solder alloy design based on quantum was proposed.

References

- [1] Mingyu Li, Chunqing Wang, Wei Zhang. *IESPT'2001, IEEE CPMT*, Beijing, August(2001)
- [2] Wang Chunqing, Li Mingyu. *Acta Metallurgica Sinica*, 13(2000), January, p.168
- [3] Tian Yanhong, Wang Chunqing. *IPACK'01*, Hawaii, July(2001)
- [4] Tian Yanhong, Wang Chunqing. *HDP'02, IEEE CPMT*, Shanghai, July(2002)
- [5] Zhao Xiujuan, Wang Chunqing. *China Welding*, 8(1999), May, p 1.
- [6] Zhao Xiujuan, Wang Chunqing. *IEEE, Trans.on Electronic Packaging*. 23(2000)

[7] Feng WF; Wang CQ; Morinaga M. *Journal of Electronic Materials* 31(2002), p 185.

[8] Feng WF; Wang CQ; Morinaga M; Yukawa H; Liu Y. *Modeling and Simulation in Materials Science and Engineering* 10(2002) p 121